J Neurophysiol 114: 3242–3254, 2015.
First published October 7, 2015; doi:10.1152/jn.00702.2015.

Goal-dependent modulation of the long-latency stretch response at the shoulder, elbow, and wrist

Jeffrey Weiler,[1,2] Paul L. Gribble,[1,2,3] and J. Andrew Pruszynski[1,2,3,4]

[1]*Brain and Mind Institute, Western University, London, Ontario, Canada;* [2]*Department of Psychology, Western University, London, Ontario, Canada;* [3]*Department of Physiology and Pharmacology, Western University, London, Ontario, Canada; and* [4]*Robarts Research Institute, Western University, London, Ontario, Canada*

Submitted 15 July 2015; accepted in final form 30 September 2015

Weiler J, Gribble PL, Pruszynski JA. Goal-dependent modulation of the long-latency stretch response at the shoulder, elbow, and wrist. *J Neurophysiol* 114: 3242–3254, 2015. First published October 7, 2015; doi:10.1152/jn.00702.2015.—Many studies have demonstrated that muscle activity 50–100 ms after a mechanical perturbation (i.e., the long-latency stretch response) can be modulated in a manner that reflects voluntary motor control. These previous studies typically assessed modulation of the long-latency stretch response from individual muscles rather than how this response is concurrently modulated across multiple muscles. Here we investigated such concurrent modulation by having participants execute goal-directed reaches to visual targets after mechanical perturbations of the shoulder, elbow, or wrist while measuring activity from six muscles that articulate these joints. We found that shoulder, elbow, and wrist muscles displayed goal-dependent modulation of the long-latency stretch response, that the relative magnitude of participants' goal-dependent activity was similar across muscles, that the temporal onset of goal-dependent muscle activity was not reliably different across the three joints, and that shoulder muscles displayed goal-dependent activity appropriate for counteracting intersegmental dynamics. We also observed that the long-latency stretch response of wrist muscles displayed goal-dependent modulation after elbow perturbations and that the long-latency stretch response of elbow muscles displayed goal-dependent modulation after wrist perturbations. This pattern likely arises because motion at either joint could bring the hand to the visual target and suggests that the nervous system rapidly exploits such simple kinematic redundancy when processing sensory feedback to support goal-directed actions.

EMG; feedback; goal-dependent activity; long-latency stretch response; reflex; movement

IT HAS BEEN PROPOSED that executing goal-directed actions involves the rapid and flexible use of sensory feedback (Scott 2004; Todorov and Jordan 2002). This position is supported by many demonstrations that muscular activity 50–100 ms after a mechanical perturbation (i.e., the long-latency stretch response) shows a range of modulation that reflects voluntary motor control (for review see Pruszynski and Scott 2012; Shemmell et al. 2010). Such modulation of the long-latency stretch response reflects sensitivity to task demands (Dietz et al. 1994; Doemges and Rack 1992a, 1992b; Hager-Ross et al. 1996; Marsden et al. 1981; Nashed et al. 2012), movement decision-making processes (Nashed et al. 2014; Selen et al. 2012; Yang et al. 2011), routing of sensory information across different muscles (Cole et al. 1984; Dimitriou et al. 2012; Marsden et al. 1981; Mutha and Sainburg 2009; Ohki and Johansson 1999; Omrani et al. 2013), as well as knowledge of the mechanical properties of the arm (Crevecoeur et al. 2012; Crevecoeur and Scott 2013; Gielen et al. 1988; Koshland et al. 1991; Kurtzer et al. 2008, 2009, 2013, 2014; Pruszynski et al. 2011a; Soechting and Lacquaniti 1988) and environment (Ahmadi-Pajouh et al. 2012; Akazawa et al. 1983; Bedingham and Tatton 1984; Cluff and Scott 2013; Dietz et al. 1994; Kimura et al. 2006; Krutky et al. 2010; Perreault et al. 2008; Pruszynski et al. 2009; Shemmell et al. 2009).

Perhaps the most studied feature of the long-latency stretch response is people's ability to intentionally modulate its amplitude. The first to demonstrate this type of goal-dependent modulation was Peter Hammond (1956). In his study, participants were told to either "resist" or "let go" in response to a mechanical perturbation that rapidly extended the elbow, stretching the biceps muscle. He found that, although the verbal instruction did not modulate the short-latency stretch response (i.e., 25–50 ms postperturbation onset), the magnitude of the long-latency stretch response was larger when participants were instructed to resist the perturbation. Since this seminal work, similar patterns of goal-dependent modulation have been shown in many muscles, including those acting at the jaw (Johansson et al. 2014), shoulder (Kurtzer et al. 2014; Nashed et al. 2012; Omrani et al. 2013; Pruszynski et al. 2008), elbow (Cluff and Scott 2013; Colebatch et al. 1979; Crago et al. 1976; Evarts and Granit 1976; Nashed et al. 2012, 2014; Omrani et al. 2013; Pruszynski et al. 2008, 2011b; Ravichandran et al. 2013; Rothwell et al. 1980; Shemmell et al. 2009), wrist (Calancie and Bawa 1985; Jaeger et al. 1982; Lee and Tatton 1982; Manning et al. 2012), finger (Capaday and Stein 1987; Cole et al. 1984; Marsden et al. 1981), and ankle (Gottlieb and Agarwal 1979; Ludvig et al. 2007).

The majority of previous studies examining goal-dependent modulation of the long-latency stretch response have focused on the assessment of individual muscles in isolation. However, purposeful movements and corrective responses typically require coordinated recruitment of several muscles spanning multiple joints. For example, even the seemingly simple act of rapidly rotating a single joint requires the recruitment of additional muscles at other joints to counteract interaction torques (Gribble and Ostry 1999). Moreover, goal-directed reaching actions can often be achieved by an infinite combination of shoulder, elbow, and wrist rotations (i.e., kinematic redundancy; see Bernstein 1967). Although there is strong evidence that the long-latency stretch response accounts for interaction torques (Kurtzer et al. 2008, 2009; Pruszynski et al.

Address for reprint requests and other correspondence: J. Weiler, Univ. of Western Ontario, The Brain and Mind Institute, 1151 Richmond St., London, ON, Canada N6A 3K7 (e-mail: jeffweilerphd@gmail.com).

 0022-3077/15 Copyright © 2015 the American Physiological Society

2011a; Soechting and Lacquaniti 1988), little is known about whether goal-dependent modulation of the long-latency stretch response reflects kinematic redundancy. As a first step in addressing this question, we used a unique 3 degree-of-freedom exoskeleton and concurrently assessed goal-dependent modulation of long-latency stretch responses from muscles that span the shoulder, elbow, and wrist while participants executed goal-directed reaches to visual targets in the horizontal plane. Beyond the ability to perturb these three joints independently, this experimental task is interesting because it is the simplest scenario that includes kinematic redundancy.

We had three specific objectives. First, we tested for goal-dependent modulation of the long-latency stretch response at the shoulder, elbow, and wrist. Although this effect has previously been demonstrated at each joint in isolation, to our knowledge no previous work has concurrently assessed modulation from muscles that articulate the three proximal joints of the upper limb. Second, we sought to identify potential relationships of the long-latency stretch responses between muscles of the upper limb. Specifically, we tested whether participants who showed relatively large goal-dependent activity within the long-latency epoch at one muscle also showed relatively large goal-dependent activity at other muscles. We also tested whether the temporal onset of goal-dependent muscle activity was constant across the muscles or reflected a proximal-to-distal gradient associated with conduction delays. Third, we examined whether modulation of the long-latency stretch response reflects multijoint characteristics of goal-directed actions—specifically, kinematic redundancy and interaction torques. In our task, mechanical perturbations applied at the elbow move the hand in such a way that the task can be successfully achieved by responding with the wrist. The reciprocal relationship is also present—mechanical perturbations at the wrist can be successfully counteracted by responses at the elbow. Thus we tested whether elbow perturbations yielded goal-dependent modulation of the long-latency stretch response in wrist muscles, and vice versa. Furthermore, because of intersegmental dynamics, rapidly flexing or extending the elbow to move the hand to the target will generate shoulder extension and flexion torques, respectively. Therefore, we also tested whether elbow perturbations generated goal-dependent long-latency stretch responses in shoulder muscles appropriate to counteract these interaction torques.

METHODS

Participants. Eighteen participants (13 men, 5 women; age range 19–33 yr) volunteered for the present experiment. All participants had normal or corrected-to-normal vision, and 17 reported being right hand dominant. Prior to data collection participants provided written informed consent. This study was approved by the Office of Research Ethics at the University of Western Ontario and was completed in accordance with the Declaration of Helsinki.

Apparatus and procedures. Participants completed the experiment with a unique 3 degree-of-freedom exoskeleton robot (Interactive Motion Technologies, Boston, MA; Fig. 1*A*). The exoskeleton allows flexion and extension at the shoulder, elbow, and wrist in a horizontal plane that intersects the shoulder joint, can apply mechanical flexion or extension loads at all aforementioned joint segments, and is equipped with encoders at each joint that measure movement kinematics (e.g., joint angles) and torque sensors to measure movement dynamics. Visual stimuli were presented downward with a 46-in. LCD monitor (60 Hz, 1,920 × 1,080 pixels, Dynex DX-46L262A12, Richfield, MN) onto a semisilvered mirror that occluded vision of the participant's arm (Fig. 1*B*). Hand position was represented by a turquoise circle (1-cm diameter), which reflected the Cartesian coordinates of the exoskeleton handle that the participants grasped. Participants were seated, and the lights in the experimental suite were extinguished for the duration of data collection.

Each trial began with the participant moving his/her hand to a red circle (i.e., home location: 2-cm diameter) that corresponded to the

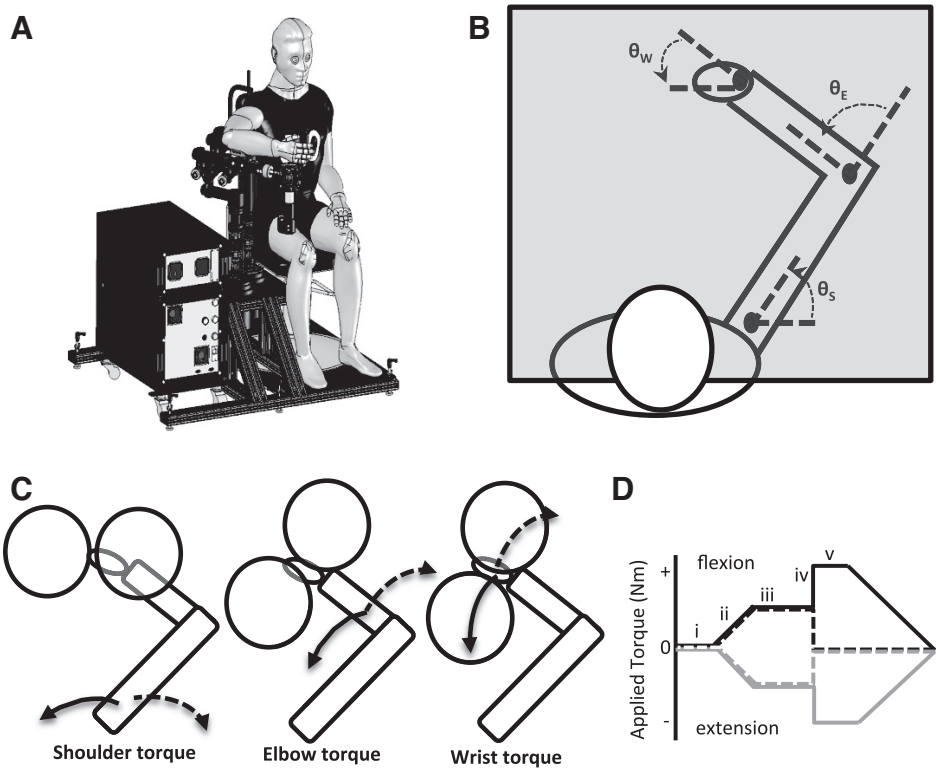

Fig. 1. *A*: schematic of the 3 degree-of-freedom exoskeleton robot that can apply flexion and extension loads at the shoulder, elbow, and wrist in the horizontal plane. *B*: top-down view of the experimental setup. A semi-silvered mirror occluded vision of the participant's hand. Flexion at the shoulder, elbow, or wrist is indicated by an increase in the magnitude of the joint angle (θ). *C*: position of the targets when the shoulder, elbow, and wrist were preloaded and perturbed by the robot. Only 1 target was presented per trial. *D*: trial timeline. *i*: Participants placed their hand at the home position (1,000 ms). *ii*: A flexion or extension ramping load was applied at the shoulder (±3 Nm), elbow (±3 Nm), or wrist (±1 Nm) (2,000 ms). *iii*: Visual hand position feedback was removed, and a white target circle was presented (2,000–4,000 ms). *iv*: A commanded step torque (i.e., perturbation) was applied at the preloaded joint (±3 Nm: shoulder and elbow; ±1 Nm: wrist) and displaced the hand toward or away from the center of the target (IN and OUT conditions, respectively). *v*: Participants moved their hand into the target after the perturbation.

hand position when the shoulder, elbow, and wrist were at 70°, 60°, and 10° of flexion, respectively. Participants were verbally instructed to adopt this joint configuration during practice trials—however, no measures were taken to enforce this specific joint configuration during data collection. After a 1,500-ms delay, a linearly increasing load was applied for 2,000 ms at the shoulder, elbow, or wrist that plateaued at a constant load of ±3 Nm at the shoulder or elbow or ±1 Nm at the wrist (i.e., the preload). When the preload plateaued, visual hand position feedback was removed (i.e., turquoise circle was extinguished). A white target circle (10-cm diameter) was then presented adjacent to the home location at a position where the preload would displace the participant's hand directly toward the center of the target or directly away from the center of the target. After the participant's hand was maintained at the home location for a random duration (1,000–2,500 ms), a commanded step torque (±3 Nm, ±3 Nm, or ±1 Nm at the shoulder, elbow, or wrist, respectively; rise time 2 ms) was applied at the preloaded joint and would displace the participant's hand into the target (IN condition) or away from the target (OUT condition; Fig. 1*C*). The participant's task was to move his/her hand into the target after the perturbation in <375 ms. The commanded step torque was removed after 1,300 ms. Performance feedback was provided after each trial. If the participant's response was inaccurate (i.e., missed the target) or too slow (i.e., took longer than 375 ms to reach the target), the target color would change from white to red to indicate an error—otherwise, the target color would change from white to green (Fig. 1*D*; see also Pruszynski et al. 2008).

Participants completed 20 trials of each of the 24 experimental conditions (3 joint segments: shoulder, elbow, wrist; 2 preloads: flexion, extension; 2 perturbation loads: flexion, extension; 2 targets: left, right) in a randomized order totaling 480 trials. Trials in which the participant moved outside the home location during the preload period were aborted and rerun later in the experiment. Prior to data collection participants completed practice trials until ~75% of their responses were successfully executed.

One participant was unable to successfully keep the hand on the home location in response to the preload during practice trials and was thus removed from the experiment.

Muscle activity. The participants' skin was abraded with rubbing alcohol, and surface EMG electrode (Delsys Bagnoli-8 system with DE-3.1 sensors, Boston, MA) contacts were covered with conductive gel. The electrodes were then placed on the bellies of six muscles [pectoralis major clavicular head (PEC; shoulder flexor), posterior deltoid (DELT; shoulder extensor), biceps brachii long head (BI; shoulder and elbow flexor, wrist supinator), triceps brachii lateral head (TRI; elbow extensor), flexor carpi ulnaris (WF; wrist flexor), and extensor carpi radialis (WE; wrist extensor)] at an orientation that runs parallel to the muscle fibers. Although BI acts to flex the shoulder and elbow as well as supinate the wrist, we analyzed its EMG activity only in relation to elbow movement (i.e., as an elbow flexor). A reference electrode was placed on the participant's left clavicle. EMG signals were amplified (gain = 10^3), band-pass filtered (20–450 Hz), and then digitally sampled at 2,000 Hz.

Data reduction. Angular positions of the shoulder, elbow, and wrist were sampled at 500 Hz. Hand position was computed by taking into account the length of each participant's arm segments (i.e., upper, lower, wrist). Kinematic data were low-pass filtered (15 Hz, 2-pass, 2nd-order Butterworth) off-line. EMG data were band-pass filtered (25–250 Hz, 2-pass, 2nd-order Butterworth) and full-wave rectified. Muscle activity was normalized to the mean EMG activity of the last 200 ms of the preload period when that muscle sample was preloaded. For example, PEC and WE muscles were normalized to their activity in conditions where the exoskeleton applied a shoulder extension and wrist flexion preload, respectively. Trials when the mechanical perturbation shortened the preloaded muscle were not analyzed (dashed lines in Fig. 1*C*). These trials comprised 12 of the 24 experimental conditions and were included so that participants could not predict the torque direction the exoskeleton would apply at perturbation onset.

Data analyses. Mean shoulder, elbow, and wrist angles as well as hand position data were computed for each participant from 200 ms before perturbation onset to 450 ms after perturbation onset. EMG activity from an individual muscle was occasionally unusable because of the surface electrode being dislodged by the robot. These data were discarded and not analyzed. Of the remaining EMG data, mean activity within the short-latency (i.e., 25–50 ms postperturbation onset) and long-latency (i.e., 50–100 ms postperturbation onset) epochs were computed for PEC (n = 17/17), DELT (n = 15/17), BI (n = 15/17), TRI (n = 16/17), WF (n = 17/17), and WE (n = 13/17) on a trial-by-trial basis. For each muscle, mean EMG values were submitted to a 2 (epoch: short latency, long latency) × 2 (condition: OUT, IN) repeated-measures ANOVA.

To determine whether the relative magnitude of participants' goal-dependent activity was consistent across muscles, we computed Spearman rank (i.e., rank-order) correlations with goal-dependent muscle activity within the long-latency epoch for all pairwise muscle combinations. Goal-dependent muscle activity was computed by determining the difference in mean EMG activity within the long-latency epoch between IN and OUT conditions from the stretched muscle of the mechanically perturbed joint.

To estimate the temporal onset of goal-dependent EMG activity for each participant, IN- and OUT-condition EMG activity from the stretched muscle of the perturbed joint was used to generate an area under a receiver operator characteristic time series from −200 to 450 ms postperturbation onset (time series ROC curve). Six time series ROC curves were computed for each participant—one for each muscle that was stretched as a function of IN and OUT conditions. Briefly, ROC curves quantify the probability that an ideal observer could discriminate between two stimuli conditions: a value of 0.5 represents chance-level discrimination, whereas a value of 0 or 1 represents perfect discrimination (Green and Swets 1966). Time series ROC curves were generated for each usable muscle sample.

We used segmented linear regression to fit the time series ROC curves in order to quantitatively determine the onset of goal-dependent muscle activity. It is important to emphasize that this regression technique is not specific to time series ROC curves—rather, segmented linear regression partitions any continuous independent variable into two separate segments that have a unique linear relationship to a dependent variable in an unbiased fashion.

Figure 2 provides an example of how the segmented linear regression was used to estimate the onset of goal-dependent activity. Figure 2*A* shows a simulated time series ROC curve (injected with Gaussian noise) that was constructed by setting the first 199 time samples to a value of 0.5 (i.e., zero discrimination ability). At *time sample 200* the ROC curve diverges toward a value of 1. We fit time series ROC curves with segmented linear regression by initially identifying the first of three consecutive time samples where the ROC value was >0.75 (i.e., "x_{end}"). Two least-squares linear regression models were then fit to the data in an iterative fashion. *Model 1* fit data from time sample x_1 to time sample x_i (restricted to a slope of 0; where x_1 is the first time sample on the ROC curve and x_i is the time sample associated with the current iteration). *Model 2* fit data from time sample x_i to $x_{end.}$ This process was iterated until $x_i = x_{end}$. For each iteration, the residual sum of squares from *model 1* and *model 2* were summed. The time sample associated with the iteration that yielded the lowest cumulative sum of squares from *models 1* and *2* served as our estimate of when the ROC curve diverged from chance discrimination. Note that Fig. 2*A* shows three functions that fit the ROC data. These functions reflect the segmented fits generated when x_i equals 100, 200, and 300. Figure 2*B* shows the cumulative sum of squares of these segmented fits and that the lowest cumulative sum of squares occurs when x_i equals 200. This iteration coincides with the time sample where the ROC curve diverges from chance levels of discrim-

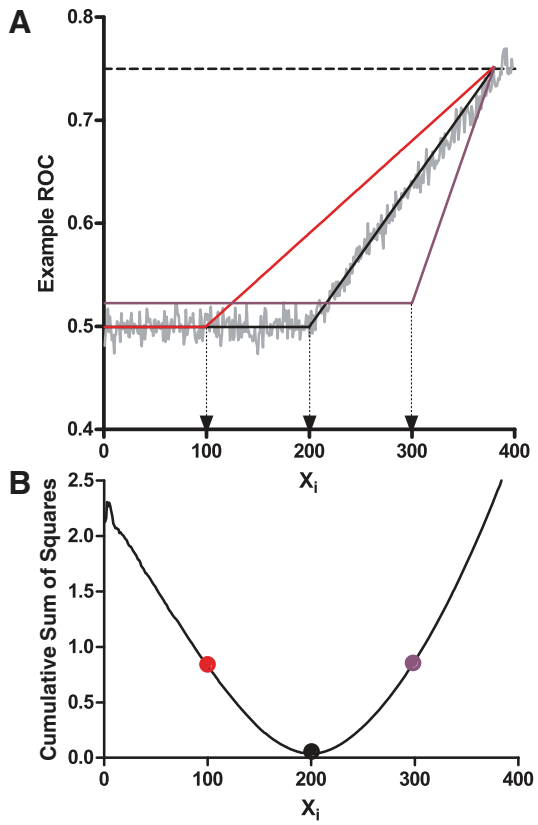

Fig. 2. *A*: example time series receiver operator characteristic (ROC) curve (gray line) where the curve diverges from chance discrimination at *sample 200*. Two independent least-square linear models are fit to the data in an iterative fashion where each successive iteration is associated with a successive time-sample. *Model 1* fits data from *sample* x_1 to *sample* x_i (restricted to a slope of 0; where x_1 is the first time sample on the ROC curve and x_i is the time sample associated with the *i*th iteration). *Model 2* fits data from *sample* x_i to *sample* x_{end} (where x_{end} is the first of 3 consecutive time samples > 0.75 on the ROC curve). This procedure is repeated until $x_i = x_{end}$. Red, black, and purple lines show how the time series ROC curve is fit when $x_i = 100$, 200, and 300, respectively. *B*: the cumulative sum of squares for *model 1* and *model 2* across all iterations of x_i. Red, black, and purple dots indicate the cumulative sum of squares of *model 1* and *model 2* when x_i equals 100, 200, and 300, respectively. The time sample associated with the iteration that yields the lowest cumulative sum of squares (i.e., $x_i = 200$) denotes the estimate of when the ROC curve diverges from chance levels of discrimination.

ination. MATLAB code that executes the segmented linear regression is provided in the Supplemental Material.[1]

The accuracy of this regression technique to estimate the onset of goal-dependent muscle activity is influenced by the amount of noise in the ROC curve and by the rate at which the ROC curves diverge from chance discrimination (i.e., rise rate). We simulated ROC curves to determine how the accuracy of the segmented linear regression is influenced when these parameters are systematically manipulated. Figure 3*A* shows two notable features of these simulations. The first is that all combinations of noise and rise time result in an overestimation of goal-dependent onset time (i.e., an estimation larger than the veridical goal-dependent onset time). The second is that the magnitude of the overestimation is dependent on the amount of noise in the ROC curve and is further accentuated based on the rise rate.

Given that ROC noise and rise rates influence the estimation of goal-dependent onset times, it is important to consider how the empirical noise and rise rate affect the ability of our regression technique to demarcate small onset timing differences between muscles. To examine this issue in the context of our data set we simulated pairs of ROC—using average noise levels and ROC rise times based on our observed data—and shifted the goal-dependent onset time of one curve relative to the other by 1-ms increments. Noise and rise rates on simulated ROC curves were set to values based on our empirical data. We then determined how many participants would be required to reliably observe imposed differences in onset times at statistical power levels of 70%, 80%, and 90%. Importantly, given our sample size our simulations indicate that we should be able to reliably identify differences in goal-dependent onset times of 4–5 ms (Table 1).

RESULTS

Features of behavior. Participants were required to quickly move their hand into a visual target after a mechanical perturbation of the shoulder, elbow, or wrist that displaced their hand either into the target (IN condition) or away from the target (OUT condition). After perturbation onset, participants took on average 15 ms and 301 ms to move their hand into the target for the IN-condition and OUT-condition trials, respectively. For OUT-condition trials participants required different amounts of time to enter the target as a function of which joint was mechanically perturbed (shoulder: 351 ms; elbow: 338 ms; wrist: 215 ms).

Prior to commencing the experiment, participants were instructed to maintain a joint configuration during the preload such that the shoulder, elbow, and wrist were at 70°, 40°, and 10° of flexion, respectively—a posture that would maintain hand position at the home location. As noted above, however, no measures were taken to enforce this posture during the experiment. Thus participants were able to select from an infinite set of upper limb joint configurations to maintain the hand at this position. This ability to utilize kinematic redundancy is highlighted in Fig. 4, which shows how the adopted joint angles of the shoulder, elbow, and wrist 2 ms prior to perturbation onset differ as a function of the preload. Visual inspection of Fig. 4, *B* and *C*, shows an inverse relationship between the elbow and wrist angle that could be used to maintain the required posture—an increase in elbow angle (i.e., increased flexion) was offset by a reduction in wrist angle (i.e., increased extension), and vice versa. We examined this finding by computing the correlation between elbow and wrist angle on a trial-by-trial basis for each participant. The computed correlation coefficients were submitted to a single-sample *t*-test, which demonstrated that the mean of these correlation coefficients (−0.26) was reliably less than zero [$t(16) = -8.06$, $P < 0.0001$].

Mean hand displacement traces when the shoulder, elbow, and wrist were perturbed are shown in Fig. 5, *A–C*. Solid and dashed lines depict the hand path after an applied extension or flexion perturbation, respectively, and blue and red traces indicate IN and OUT conditions, respectively. Note that the paths of the IN and OUT condition traces overlap for the initial part of the movement. This initial overlap was expected because the exoskeleton applied the same load at perturbation onset. The traces then diverge as participants counteracted the unpredictable perturbation and moved toward the presented target.

Changes in shoulder, elbow, and wrist angles following a mechanical perturbation applied at any of the aforementioned joint segments are depicted in Fig. 5*D*. More specifically, the

[1] Supplemental Material for this article is available online at the Journal website.

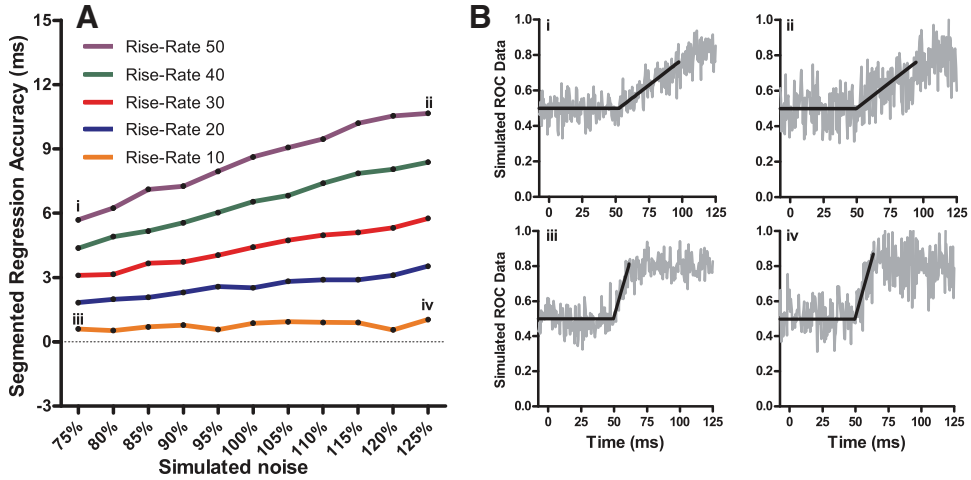

Fig. 3. *A*: accuracy of the segmented linear regression to estimate the onset of goal-dependent EMG activity with varying amounts of noise and rise rates of the time series ROC curve. Each data point reflects the mean estimate of goal-dependent onset times from 1,500 simulated ROC curves where the true onset of goal dependence was set at 50 ms. Values > 0 reflect estimations > 50 ms. We set "100% noise" to the standard deviation of our experimental ROC data from 25 ms before perturbation onset to 25 ms after perturbation across all participants because values on the ROC curve within this epoch should theoretically be 0.5. Simulated rise rates reflect the range of rise rates observed in the experimental ROC data. The mean rise rate from the experimental data was 19 ms. *B*, *i–iv*: exemplar simulated time series ROC curves from the 4 extremes of the manipulated noise and rise rate combinations observed in *A* to demonstrate how the ROC curve is influenced as a function of these 2 parameters.

figure shows how the changes in joint angles differ as a function of IN and OUT conditions. Similar to Fig. 5, *A–C*, IN- and OUT-condition traces on each panel initially overlap, which reflects how a mechanical perturbation initially influenced joint angles. OUT-condition traces diverge from their IN-condition counterparts as participants counteracted the applied perturbation that displaced their hand away from the presented target. Of note is the kinematically redundant relationship between the elbow and wrist. The OUT-condition traces in Fig. 5*Dviii* show that when the elbow was mechanically perturbed the wrist was quickly incorporated (i.e., ~150 ms after perturbation) into a movement that transported the hand to the target. The OUT-condition traces on Fig. 5*Dvi* show a similar effect for elbow movement in response to a perturbation applied to the wrist—that is, the elbow quickly assisted movement of the hand toward the goal location after a perturbation applied to the wrist.

Table 1. *Summary of statistical power simulations*

Difference Between 2 Goal-Dependent Onset Times, ms	No. of Participants Required to Identify Onset Differences at Desired Power of:		
	70%	80%	90%
10	3	3	4
9	3	4	5
8	4	4	5
7	4	5	6
6	5	6	8
5	6	8	10
4	9	11	15
3	15	19	25
2	33	41	54
1	126	160	211

Results were generated with 10,000 simulations per onset difference and desired power combination. Simulated time series receiver operator characteristic (ROC) curves used the mean noise and rise time values observed in our experimental data.

Stretched muscles display rapid goal dependence. Our first objective was to test whether the stretched muscle that articulated the mechanically perturbed joint displayed goal-dependent long-latency stretch responses. Figure 6, *A* and *B*, show an exemplar participant's trial-by-trial TRI EMG activity after elbow flexion perturbations for IN (Fig. 6*A*) and OUT (Fig. 6*B*) conditions. Note the increased EMG activity within the long-latency epoch for the OUT- compared with IN-condition trials. Group EMG results for the six stretched muscles are shown in Fig. 7. Figure 7, *A–F*, specifically contrast the group mean EMG activity for IN and OUT conditions from −25 ms before perturbation onset to 125 ms after the perturbation, whereas Fig. 7, *G–L*, depict participant mean EMG activity within the short- and long-latency epochs as a function of IN and OUT conditions. Repeated-measures ANOVAs revealed reliable main effects of epoch and condition as well as their reliable interaction across all muscles. Interactions were decomposed with paired-sample *t*-tests. Mean EMG activity for all muscles within the short-latency epoch did not differ between IN and OUT conditions. In contrast, mean EMG activity within the long-latency epoch was reliably larger for OUT conditions compared with their IN-condition counterparts for all six muscles. Test statistics, degrees of freedom, and *P* values for all post hoc contrasts are provided in Table 2. The same pattern of results was observed when post hoc contrasts were completed with a nonparametric (i.e., Wilcoxon signed rank) test.

Magnitude and temporal relationships of goal-dependent activity between muscles. Our second objective had two components. We wanted to determine whether the magnitude of participants' goal-dependent activity within the long-latency epoch from one muscle was related to the magnitude of their goal-dependent activity within the long-latency epoch from the other muscles. To make this assessment, we computed Spearman rank correlation coefficients for all pairwise muscle combinations (Table 3). This analysis revealed positive correlations for all pairwise comparisons that were particularly strong for

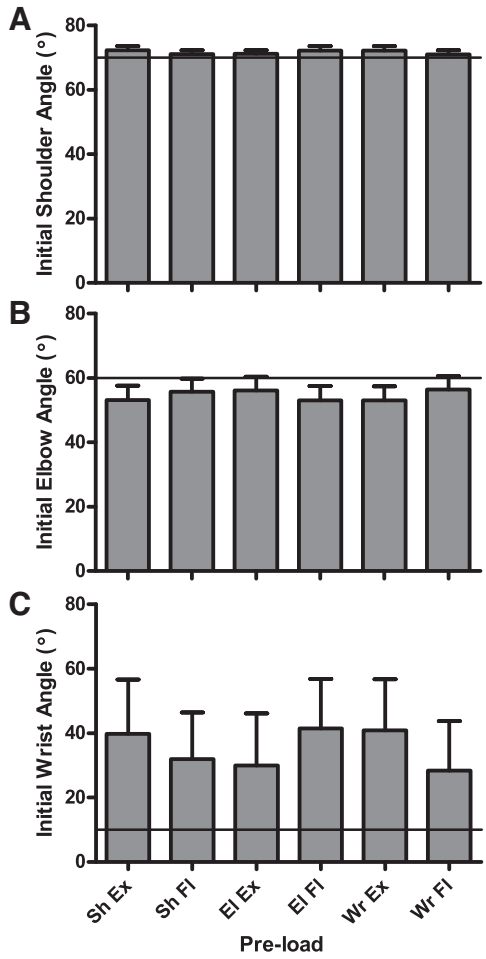

Fig. 4. Shoulder (*A*), elbow (*B*), and wrist (*C*) joint angles 2 ms prior to perturbation onset plotted as a function of preload (Sh, shoulder; El, elbow; Wr, wrist; Ex, extension; Fl, flexion). Horizontal black lines indicate the instructed joint position for the respective joint segments. Error bars represent 1 SD.

muscles at the same joint (i.e., PEC and DELT, BI and TRI, and WF and WE).

We also sought to determine the temporal onset of goal-dependent activity across muscles. We did so by using segmented linear regression to fit the time series ROC curves that were computed for each muscle sample (see METHODS). Figure 8*A* depicts one time series ROC curve of an exemplar muscle sample (WF) fit with our regression technique. The estimated onset time of goal-dependent activity for this muscle sample was 73 ms after perturbation onset. Estimates of goal-dependent onset times were computed for all muscle samples (Fig. 8*B*) and submitted to an independent-samples one-way ANOVA to determine whether these times differed as a function of muscle. Results of this analysis yielded no reliable differences [$F(5,86) = 0.66$, $P = 0.67$]. Although no differences were observed, it is important to note that several of these estimates fall well outside the long-latency epoch and were obtained from muscles that did not show goal-dependent long-latency stretch responses. We reran this analysis with only the estimates from muscles that showed reliable mean EMG differences (i.e., $P < 0.05$) between IN and OUT conditions within the long-latency epoch (Fig. 8*B*). Results of this analysis also yielded no reliable differences [$F(5,48) = 0.52$ $P = 0.76$]. The mean estimate for the onset of goal-dependent activity across muscles was 64 ms (SD = 16) after perturbation onset.

We further tested whether goal-dependent onset times differed across muscles by identifying a total of 22 elbow-nonelbow muscle pairs (e.g., BI and PEC, TRI and WE) across all participants that both displayed reliable (i.e., $P < 0.05$) goal-dependent long-latency stretch responses after an elbow perturbation. ROC curves were generated for these muscle samples, each fit with our segmented linear regression technique to estimate the onset of goal-dependent activity and then compared with a paired-sample *t*-test. We again found no reliable difference in goal-dependent onset time between elbow muscles and muscles at the shoulder or wrist after an elbow perturbation [$t(21) = 0.78$, $P = 0.48$]. The mean estimate for the onset of goal-dependent activity of elbow and nonelbow muscles following an elbow perturbation was 66 ms (SD = 16) after perturbation onset.

Multijoint modulation of long-latency stretch response. Our third objective was to examine whether modulation of the long-latency stretch response reflected two multijoint characteristics of goal-directed actions: kinematic redundancy and interaction torques. In terms of kinematic redundancy, we sought to determine whether modulation of the long-latency stretch response of elbow muscles would display an appropriate pattern of goal-dependent activity when the wrist had been mechanically perturbed. We also sought to address the reciprocal relationship—that is, to determine whether long-latency stretch response of wrist muscles would display appropriate goal-dependent activity after mechanical perturbations of the elbow.

Figure 9*A* shows the mean EMG profile of TRI activity in response to a perturbation that flexed the wrist, whereas Fig. 9*D* shows the mean EMG profile of BI activity following a perturbation that extended the wrist. Both panels contrast the EMG activity in response to a perturbation that displaced the hand into the target (IN condition) and away from the target (OUT condition). Paired-sample *t*-tests revealed that long-latency stretch responses had larger activity for the OUT condition compared with their IN-condition counterpart for both TRI [$t(15) = 3.06$, $P = 0.008$] and BI [$t(14) = 2.30$, $P = 0.037$]. A similar effect was observed for muscles that articulate the wrist when the elbow was mechanically perturbed. Figure 9*B* depicts activity of the WE in response to a mechanical perturbation that flexed the elbow, whereas Fig. 9*E* depicts WF activity following a perturbation that extended the wrist. Results show that long-latency stretch responses were larger for OUT conditions compared with IN conditions for both WE [$t(12) = 2.21$, $P = 0.047$] and WF [$t(16) = 3.22$, $P = 0.005$].

It is possible that these findings were due to rapid muscular cocontraction following a perturbation at an adjacent joint that displaced the hand away from the target. For example, after a wrist extension perturbation that moved the hand away from the target, it is possible that WF and WE rapidly cocontracted. To test this possibility, we performed four additional comparisons that contrasted activity of the long-latency stretch response when the perturbation displaced the hand in or away from the target. Specifically, we compared WF long-latency activity following an elbow flexion perturbation; WE long-latency activity following an elbow extension perturbation; BI long-latency activity following a wrist flexion perturbation; and TRI long-latency activity following a wrist extension

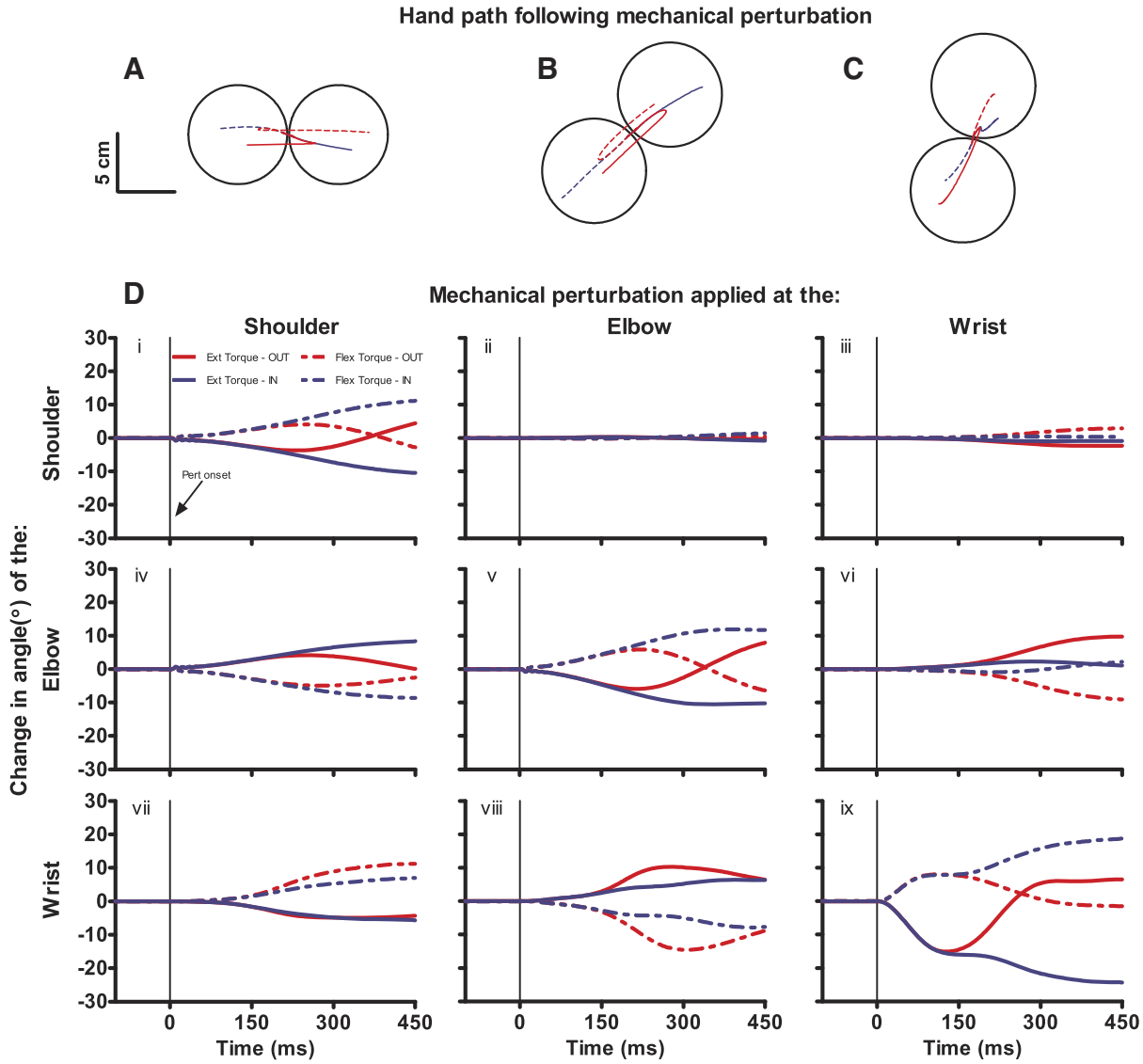

Fig. 5. *A–C*: hand paths produced when the perturbation was applied to the shoulder, elbow, and wrist, respectively. Extension and flexion perturbations are denoted by solid and dashed lines, respectively. IN and OUT conditions are denoted by blue and red lines, respectively. *D*: changes in shoulder (*top*), elbow (*middle*), and wrist (*bottom*) angles in response to mechanical perturbations applied to the shoulder (*left*), elbow (*center*), or wrist (*right*). Flexion and extension perturbations are denoted via dashed and solid lines, respectively. IN and OUT conditions are shown by blue and red traces, respectively.

perturbation. Note that these comparisons are of the antagonist muscles from the conditions previously tested. Results of these comparisons showed either that there was no reliable difference in the activity of the long-latency stretch response between OUT and IN conditions [BI: $t(14) = -1.47$, $P = 0.16$; WF: $t(16) = -1.38$, $P = 0.19$; WE: $t(12) = 1.09$, $P = 0.30$] or that the long-latency stretch response was reliably smaller for OUT-condition trials relative to their IN-condition counterpart [TRI: $t(15) = -3.16$, $P = 0.006$]. Thus long-latency stretch responses of wrist muscles displayed selective goal-dependent activity when the elbow was mechanically perturbed in a manner that assisted in transporting the hand to the goal location. The same was also true for long-latency stretch responses of elbow muscles when the wrist was mechanically perturbed.

In terms of interaction torques, we sought to determine whether elbow perturbations generated goal-dependent long-latency stretch responses in shoulder muscles appropriate to counteract interaction torques (see also Kurtzer et al. 2014). Figure 9*C* shows the mean EMG profile of DELT activity in response to a perturbation that flexed the elbow, whereas Fig. 9*F* shows the mean EMG profile of PEC activity following a perturbation that extended the elbow. Both panels contrast the EMG activity in response to a perturbation that displaced the hand into the target (IN condition) and away from the target (OUT condition). Paired-sample *t*-tests demonstrated that when the elbow was perturbed into flexion DELT long-latency stretch responses were reliably larger for OUT-condition trials compared with their IN-condition counterparts [$t(14) = 3.11$, $P = 0.008$]. Furthermore, when the elbow was perturbed into extension PEC long-latency stretch responses were also larger for OUT-condition trials compared with IN-condition trials [$t(16) = 2.91$, $P = 0.01$]. These shoulder responses are appropriate to counteract interaction torques generated by the elbow motion used by participants to transport their hand into the target. To rule out general cocontraction of all

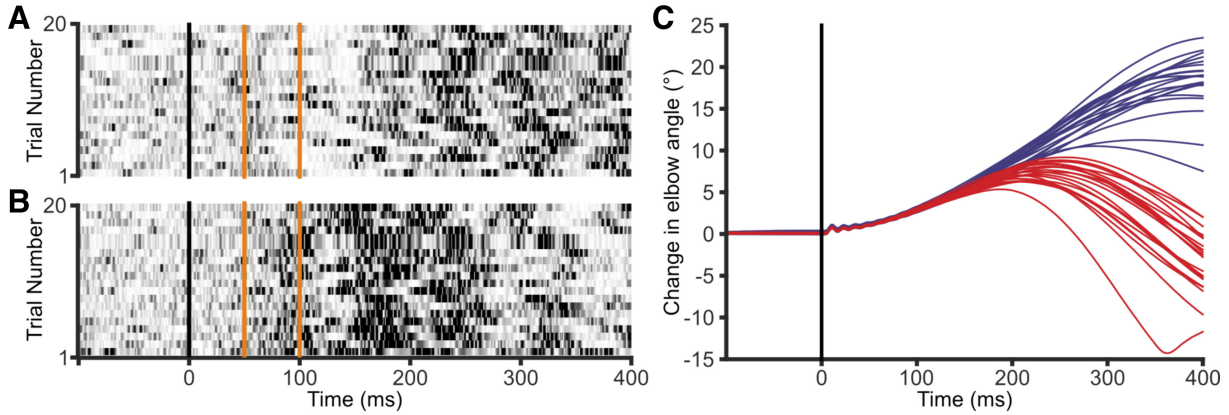

Fig. 6. *A* and *B*: an exemplar participant's triceps brachii lateral head (TRI) EMG data from trials in which an elbow flexion perturbation moved the hand into (IN condition; *A*) or away from (OUT condition; *B*) the target. Dark colors reflect greater activity compared with light colors, and each row depicts data from a single trial. Black vertical line denotes perturbation onset, and orange vertical lines demarcate the long-latency epoch. *C*: traces of elbow angle over time after elbow flexion perturbations for all trials shown in *A* and *B*. Black vertical line denotes perturbation onset, and blue and red traces reflect IN and OUT conditions, respectively.

shoulder muscles in response to elbow movement, we contrasted OUT- and IN-condition DELT long-latency stretch responses when the elbow was perturbed into extension and OUT- and IN-condition PEC long-latency stretch responses when the elbow was perturbed into flexion. Results showed that long-latency stretch responses of the DELT were reliably smaller for the OUT condition compared with their IN-condition counterparts when the elbow was perturbed into extension [$t(14) = -2.15$, $P = 0.05$], whereas there was no reliable difference between OUT and IN conditions for the PEC long-latency stretch responses following a perturbation that flexed the elbow [$t(16) = -1.46$, $P = 0.16$]. These findings again demonstrate a selective and appropriate modulation of the long-latency stretch response to complete the goal-directed action.

DISCUSSION

We assessed modulation of short-latency and long-latency stretch responses from shoulder, elbow, and/or wrist muscles while participants responded to mechanical perturbations by placing their hand into visually defined spatial targets. The targets were strategically placed such that the same perturbation displaced the hand directly into or away from a target—a manipulation previously shown to elicit robust goal-dependent activity in the long-latency epoch at the shoulder and elbow (Pruszynski et al. 2008). Unlike previous studies using this approach, we focused on the concurrent modulation across multiple muscles that span the three proximal joints of the upper limb. Important in this effort was a unique robotic exoskeleton that can measure and perturb movement at the shoulder, elbow, and wrist while the participant's hand is

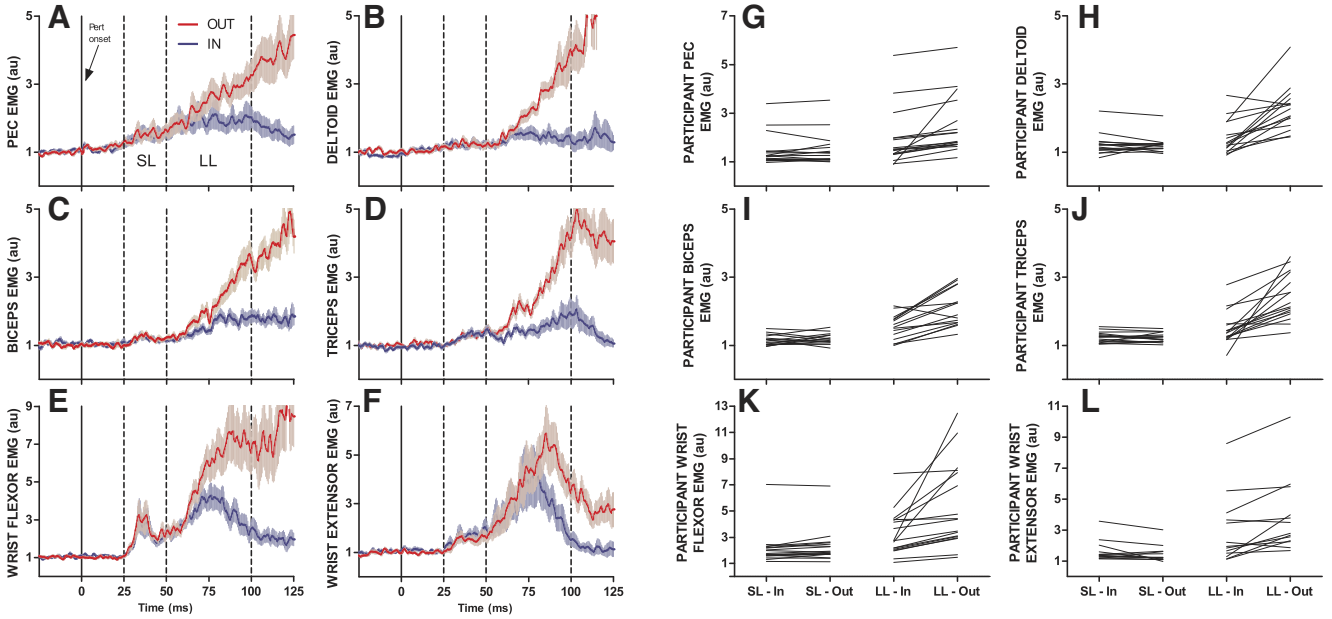

Fig. 7. EMG activity from the stretched muscle that articulated the perturbed joint. *A–F*: group mean EMG activity for IN and OUT conditions. Shading around EMG activity represents 1 SE. *G–L*: mean EMG activity for each participant within the short-latency (SL) and long-latency (LL) epochs as a function of IN and OUT conditions. Muscles that articulate the shoulder, elbow, and wrist are presented at *top*, *middle*, and *bottom*, respectively. Note that no muscle shows a reliable difference between IN and OUT conditions within the short-latency epoch whereas EMG activities within the long-latency epoch are larger for OUT conditions compared with their IN-condition counterparts for all muscles. PEC, pectoralis major clavicular head; au, arbitrary unit.

Table 2. *Statistics of EMG comparisons between OUT and IN conditions from stretched muscles*

Stretched Muscle	Degrees of Freedom	Short-Latency Stretch Response		Long-Latency Stretch Response	
		t-Ratio	*P* Value	*t*-Ratio	*P* Value
PEC	16	−1.12	0.28	3.68	0.002
DELT	14	0.10	0.92	3.48	0.004
BI	14	−0.38	0.71	3.59	0.003
TRI	15	0.28	0.78	2.80	0.01
WF	16	−1.84	0.08	2.98	0.009
WE	12	−1.55	0.15	2.54	0.03

Positive *t*-ratio reflects larger EMG activity for OUT compared to IN condition. PEC, pectoralis major clavicular head; DELT, posterior deltoid; BI, biceps brachii long head; TRI, triceps brachii lateral head; WF, flexor carpi ulnaris (wrist flexor); WE, extensor carpi radialis (wrist extensor).

constrained to move in a horizontal plane at the level of the shoulder. We report four principal findings. First, goal-dependent modulation of the mechanically stretched muscle was never present in the short-latency epoch but always present in the long-latency epoch. Second, the relative magnitude of a participant's goal-dependent activity at one muscle was positively correlated with the relative magnitude of the goal-dependent activity at the other muscles. Third, the temporal onset of goal-dependent activity was statistically indistinguishable across the proximal-to-distal muscles of the arm. And fourth, goal-dependent activity was coordinated across muscles spanning the elbow and wrist joint such that mechanical perturbations applied at one joint were readily countered by responses at the other joint. Taken together, our results strengthen the claim that long-latency stretch responses are flexibly coordinated across muscles to support goal-directed actions.

Goal-dependent modulation of mechanically stretched muscles. We observed both short-latency and long-latency stretch responses in muscles that were lengthened by the mechanical perturbation. Consistent with many previous studies, we found no evidence of goal-dependent modulation in the short-latency epoch for any muscle (for review see Pruszynski and Scott 2012). That is, we found no reliable difference in the evoked muscle response when contrasting the IN and OUT conditions for the same applied mechanical perturbation. Despite the lack of modulation observed with our task, it is important to emphasize that the short-latency stretch response is not immutable. Indeed, many studies have shown substantial changes in the sensitivity of the short-latency stretch response at the transition between posture and movement (Duysens et al. 1993; Komiyama et al. 2000; Mortimer et al. 1981) and over the course of cyclical movements such as gait (Akazawa et al. 1982; Capaday and Stein 1986; Forssberg et al. 1975; Zehr and Chua 2000; Zehr and Haridas 2003). In fact, previous work has shown that directly reinforcing the magnitude of the H reflex—an electrical analog of the short-latency stretch response—over several days or weeks can yield progressive increases or decreases in its magnitude (Carp et al. 2006; Chen et al. 2006; Christakos et al. 1983; Thompson et al. 2009; Wolf and Segal 1996; Wolpaw 1987; Wolpaw et al. 1983).

Table 3. *Spearman rank correlation coefficients for magnitude of participant goal-dependent activity between muscles*

Muscle	DELT	BI	TRI	WF	WE
PEC	0.454 0.09 (15)	0.075 0.79 (15)	0.282 0.29 (16)	0.512 0.04 (17)	0.560 0.05 (13)
DELT		0.308 0.31 (13)	0.314 0.25 (15)	0.543 0.04 (15)	0.413 0.18 (12)
BI			0.631 0.02 (14)	0.493 0.06 (15)	0.269 0.37 (13)
TRI				0.238 0.37 (16)	0.170 0.58 (13)
WF					0.648 0.02 (13)

Top value in cells reflects the computed Spearman correlation coefficient. Bottom values in cells reflect the *P* value and no. of participants (in parentheses) associated with each correlation.

In contrast to the short-latency stretch response, all muscles showed robust goal-dependent modulation in the long-latency epoch, starting ~65 ms after perturbation onset. This difference between the short-latency and long-latency stretch responses likely reflects differences in the neural circuitry that underlies the muscle activity in these epochs (for reviews see Matthews 1991; Pruszynski 2014; Pruszynski and Scott 2012; Shemmell et al. 2010). Briefly, the timing of the short-latency stretch response, appearing on the muscle ~25–50 ms after perturbation onset, requires that it engage a spinal circuit mediated by relatively large-diameter afferent fibers (Pierrot-Desilligny and Burke 2005). The neural basis of the long-latency stretch response is more complicated (for review see Pruszynski and Scott 2012), as it likely reflects the temporal overlap of several sources at multiple levels of the neuraxis, including spinal cord, brain stem, and cortex (Cheney and Fetz 1984; Evarts and Tanji 1976; Grey et al. 2001; Kimura et al. 2006; Kurtzer et al. 2010, 2014; Lourenço et al. 2006; Matthews 1984; Matthews and Miles 1988; Omrani et al. 2014; Pruszynski 2014; Pruszynski et al. 2011a; Schuurmans et al. 2009; Shemmell et al. 2009). An added complication is that these distinct neural generators may have unique or overlapping functional capacity. For example, it has been demonstrated that the long-latency stretch response can be functionally segregated into two components: one that is sensitive to task goals but not the preperturbation load environment and another that is sensitive to the load environment but not task goals (Pruszynski et al. 2011b). Interestingly, follow-up work revealed that both of the goal-dependent and load-dependent components account for the intersegmental dynamics of the arm (Kurtzer et al. 2014).

The neural basis of goal-dependent modulation within the long-latency epoch—the focus of the present study—is also largely unknown. One possibility is that such modulation reflects processing within a transcortical pathway centered on primary motor cortex (for reviews see Matthews 1991; Pruszynski 2014; Pruszynski and Scott 2012). Neurons in

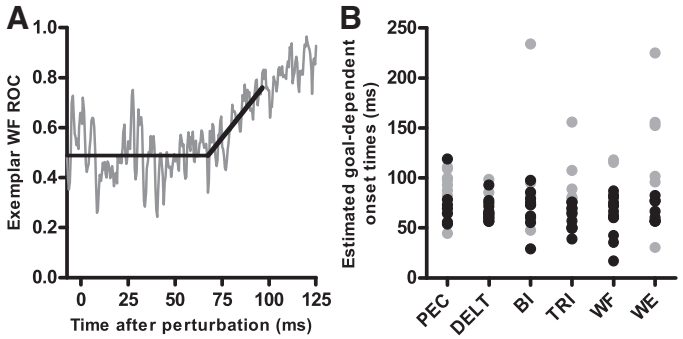

Fig. 8. *A*: time series ROC curve from an exemplar muscle sample [flexor carpi ulnaris (WF; wrist flexor)]. The goal-dependent onset time for this sample was estimated to be 73 ms after perturbation onset. *B*: estimates of goal-dependent onset time from all muscle samples are shown as gray dots, whereas black dots represent the estimates of goal-dependent onset times from muscle samples that demonstrated reliable goal-dependent activity within the long-latency epoch. One estimated biceps brachii long head (BI) onset time was not estimated because one participant's BI ROC curve never exceeded 0.75. DELT, posterior deltoid; WE, extensor carpi radialis (wrist extensor).

primary motor cortex respond quickly to mechanical perturbations (Cheney and Fetz 1984; Evarts and Fromm 1977; Evarts and Tanji 1976; Picard and Smith 1992; Pruszynski et al. 2011a, 2014; Wolpaw 1980), and these responses are sensitive to the instructed action (Evarts and Tanji 1976; Omrani et al. 2014; Pruszynski et al. 2014). Recent work using a paradigm similar to the one used in our experiment has shown that, after a mechanical perturbation, neurons in the monkey primary motor cortex are modulated as a function of the movement goal and that such modulation occurs early enough to generate changes in muscle activity in the long-latency epoch (Pruszynski et al. 2014). It is important to note, however, that although neurons in primary motor cortex respond to a mechanical perturbation within 20 ms of perturbation onset, goal-dependent activity does not arise until ~40 ms after perturbation (Evarts and Tanji 1976; Omrani et al. 2014; Pruszynski et al. 2014). This transition from goal-independent to goal-dependent activity may result from intrinsic processing within primary motor cortex or an efference copy of processing performed in other cortical or subcortical structures. One possible structure is the dentate nucleus of the cerebellum. Dentate neurons show goal-dependent activity ~30 ms after perturbation onset (Strick 1983), and cooling this area yields a reduction in perturbation-related responses in primary motor cortex (Hore and Vilis 1984). Another possibility is oligosynaptic circuits in the spinal cord. Spinal interneurons are well suited to generate goal-dependent activity within the long-latency epoch as they rapidly receive sensory information from the periphery and descending modulatory input from the brain stem and cerebral cortex (Pierrot-Deseilligny and Burke 2005). Indeed, a biologically realistic model of the spinal circuitry that receives relatively simple control inputs can generate stabilizing responses to force perturbations (Raphael et al. 2010), akin to the long-latency stretch response.

Goal-dependent modulation of long-latency stretch response across muscles. Many studies have demonstrated goal-dependent modulation of the long-latency stretch response from muscles at the shoulder, elbow, and/or wrist (for review see Pruszynski and Scott 2012). To our knowledge, however, our work is the first to concurrently analyze goal-dependent modulation from muscles at all these joints. Simultaneously recording and analyzing responses from multiple muscles that span multiple joints yielded two notable findings.

We found that the relative magnitude of goal-dependent modulation was consistent across muscles. That is, a participant who showed a relatively large (or small) difference between evoked responses for IN and OUT conditions at one muscle tended to also show a relatively large (or small) difference at the other muscles. Such a finding suggests that the neural network that supports the long-latency stretch response receives a common goal-dependent input that is used to modulate all muscle activity. Neurons in primary motor cortex are a possible target for such a common input as they often make functional connections with more than one muscle spanning several joints (Buys et al. 1986; Fetz and Cheney 1980; McKiernan et al. 1998). Further studies should investigate this possibility. In addition to our analyses, which focused on mean EMG responses across muscle samples, it would be interesting to test whether and how goal-dependent activity is structured on a trial-by-trial basis. For example, in terms of kinematic redundancy, muscles that both contribute to task success may show a reciprocal amount of goal-dependent activity on a trial-by-trial basis. We were unable to reliably assess this type of relationship because we collected 20 trials per experimental condition and previous work suggests that ~40 trials are required to reliably correlate long-latency stretch response at the single-trial level (Pruszynski et al. 2011b).

We also found that goal-dependent activity began ~65 ms after perturbation onset regardless of whether the muscle

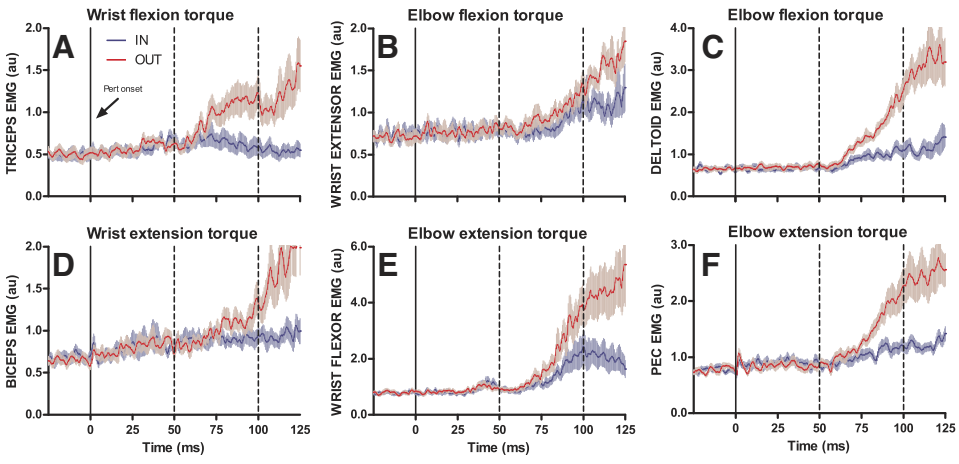

Fig. 9. *A* and *D*: TRI and BI activity when the wrist was mechanically flexed and extended, respectively. Panels contrast EMG activity as a function of IN (blue traces) and OUT (red traces) conditions, and the region between the vertical dashed lines is the long-latency epoch. Shading around EMG activity represents 1 SE. *B* and *E*: same format as *A* and *D* but for WE and WF when the elbow was mechanically flexed and extended, respectively. *C* and *F*: same format as *A* and *D* but for DELT and PEC when the elbow was mechanically flexed and extended, respectively.

spanned the shoulder, elbow, or wrist. Our finding runs counter to previous work demonstrating that shoulder muscles are activated prior to elbow muscles during voluntary reaching movements (Karst and Hasan 1991) and was unexpected given afferent and efferent conduction delays. Conduction velocities of ~50–70 m/s (Ingram et al. 1987; Macefield et al. 1989) and the ~30- to 50-cm distance between the shoulder and wrist muscles would yield goal-dependent activity at shoulder muscles 9–20 ms prior to wrist muscles. Although this asynchrony may be slightly overestimated because we have not accounted for all physiological details (e.g., precise nerve innervation pattern; neuromuscular architecture), it is important to note that even small conduction delays could have functional consequences for the execution of goal-directed actions, which can require temporal precision on the order of 1–2 ms (Hore and Watts 2011). Our results indicate that the neural network that supports the long-latency stretch response may account for conduction delays by sending goal-dependent signals to distal muscles prior to proximal muscles—a process that apparently sacrifices the absolute response latency of muscles spanning proximal joints for a coordinated response across muscles spanning multiple joints. Although the neural implementation of this process is unknown, the cerebellum is a likely node, as individuals with cerebellar damage display abnormal timing of the long-latency stretch response compared with healthy control subjects (Kurtzer et al. 2013). Indeed, a hallmark of cerebellar damage is the inability to coordinate voluntary movement (e.g., ataxia, dysdiadochokinesia, dysmetria), and previous functional brain imaging, patient and animal studies have shown that this region is involved in motor tasks that require accurate timing (Conrad and Brooks 1974; Ivry and Keele 1989; Vilis and Hore 1980) and precise joint coordination (Bastian et al. 1996; Diedrichsen et al. 2007).

Flexible routing of sensory feedback. Previous findings have shown that salient sensory information can elicit goal-dependent activity in the long-latency epoch within muscles that were not mechanically stretched. For example, Marsden and colleagues (1981), in their "tea-cup experiment," found goal-dependent activity in right arm muscles when a participant's left arm was pulled forward. If the participant was holding an adjacent table with the right hand, long-latency stretch responses were generated in the right triceps after the perturbation, which helped stabilize the body. However, if the participant was holding an object in the right hand, long-latency stretch responses were no longer elicited in the right triceps but instead were generated in the right biceps, which helped keep the object stable. Similar findings have been demonstrated in finger muscles during object manipulation (Cole et al. 1984), in facial muscles during speech (Abbs and Gracco 1984), and in arm muscles during bimanual coordination (Dimitrou et al. 2012; Mutha and Sandberg 2009; Omrani et al. 2013).

We observed a similar phenomenon whereby goal-dependent activity in the long-latency epoch was elicited in muscles that were not directly stretched by the mechanical perturbation. In our experiment the visual targets were placed such that participants could succeed at the task by counteracting perturbations applied at the elbow with movement at the wrist, and vice versa. Participants exploited this relatively simple kinematically redundant relationship. Behavioral analysis revealed that the unperturbed joint began to transport the hand toward the target ~150 ms after perturbation onset. Critically, the magnitude of the long-latency stretch response increased in wrist (or elbow) muscles when an applied elbow (or wrist) perturbation displaced the hand away from the target. The response at the unperturbed joint was not merely an unselective increase in activity to stiffen the joint (i.e., cocontraction)—rather, long-latency stretch responses selectively displayed goal-dependent activity only in muscles that were appropriate for transporting the hand toward the target.

Our results motivate testing whether long-latency stretch responses can account for more complex redundancy scenarios that arise, and can be exploited, during voluntary arm movements. When aiming a gun, for example, repeatedly pointing the barrel toward the target could be achieved by selecting the same set of shoulder, elbow, and wrist angles on each shot—a solution that does not exploit kinematic redundancy. However, Scholz and colleagues (2000) demonstrated that participants do exploit kinematic redundancy in this type of task. That is, participants selected various joint configurations that were structured so that the net effect kept the gun's barrel pointed at the target. Demonstrating that the long-latency stretch response can account for the full scope of the arm's kinematic redundancy would be an important step toward further establishing that executing goal-directed actions involves the rapid and flexible use of sensory feedback.

GRANTS

J. A. Pruszynski was supported during this work through Natural Sciences and Engineering Research Council of Canada (NSERC). P. L. Gribble was supported during this work through NSERC and Canadian Institutes of Health Research (CIHR).

DISCLOSURES

No conflicts of interest, financial, or otherwise, are declared by the author(s).

AUTHOR CONTRIBUTIONS

Author contributions: J.W. and J.A.P. conception and design of research; J.W. performed experiments; J.W. analyzed data; J.W., P.L.G., and J.A.P. interpreted results of experiments; J.W. prepared figures; J.W. drafted manuscript; J.W., P.L.G., and J.A.P. edited and revised manuscript; P.L.G. and J.A.P. approved final version of manuscript.

REFERENCES

Abbs JH, Gracco VL. Control of complex motor gestures: orofacial muscles responses to load perturbations of lip during speech. *J Neurophysiol* 51: 705–723, 1984.

Ahmadi-Pajouh MA, Towhidkhah F, Shadmehr R. Preparing to reach: selecting an adaptive long-latency feedback controller. *J Neurosci* 32: 9537–9545, 2012.

Akazawa K, Aldridge JW, Steeves JD, Stein RB. Modulation of stretch reflexes during locomotion in the mesencephalic cat. *J Physiol* 329: 553–567, 1982.

Akazawa K, Milner TE, Stein RB. Modulation of reflex EMG and stiffness in response to stretch of human finger muscle. *J Neurophysiol* 49: 16–27, 1983.

Bastian AJ, Martin TA, Keating JG, Thach WT. Cerebellar ataxia: abnormal control of interaction torques across multiple joints. *J Neurophysiol* 76: 492–509, 1996.

Bedingham W, Tatton WG. Dependence of EMG responses evoked by imposed wrist displacements on pre-existing activity in the stretched muscles. *Can J Neurol Sci* 11: 272–280, 1984.

Bernstein NA. *The Co-ordination and Regulation of Movements*. Oxford, UK: Pergamon, 1967.

Buys EJ, Lemon RN, Mantel GW, Muir RB. Selective facilitation of different hand muscles by single corticospinal neurons in the conscious monkey. *J Physiol* 381: 529–549, 1986.

Calancie B, Bawa P. Voluntary and reflexive recruitment of flexor carpi radialis motor units in humans. *J Neurophysiol* 53: 1194–1200, 1985.

Capaday C, Stein RB. Amplitude modulation of the soleus H-reflex in the human during walking and standing. *J Neurosci* 6: 1308–1313, 1986.

Capaday C, Stein RB. A method for simulating the reflex output of a motoneuron pool. *J Neurosci Methods* 21: 91–104, 1987.

Carp JS, Tennissen AM, Chen XY, Wolpaw JR. H-reflex operant conditioning in mice. *J Neurophysiol* 96: 1718–1727, 2006.

Chen Y, Chen XY, Jakeman LB, Chen L, Stokes BT, Wolpaw JR. Operant conditioning of H-reflex can correct a locomotor abnormality after spinal cord injury in rats. *J Neurosci* 29: 12537–12543, 2006.

Cheney PD, Fetz EE. Corticomotoneuronal cells contribute to long-latency stretch reflexes in the rhesus monkey. *J Physiol* 349: 249–272, 1984.

Christakos CN, Wolf H, Meyer-Lohmann J. The "M2" electromyographic response to random perturbations of arm movements is missing in long-trained monkeys. *Neurosci Lett* 41: 295–300, 1983.

Cluff T, Scott SH. Rapid feedback responses correlate with reach adaptation and properties of novel upper limb loads. *J Neurosci* 33: 15903–15914, 2013.

Cole KJ, Gracco VL, Abbs JH. Autogenic and nonautogenic sensorimotor actions in the control of multiarticulate hand movements. *Exp Brain Res* 56: 582–585, 1984.

Colebatch JG, Gandevia SC, McCloskey DI, Potter EK. Subject instruction and long latency reflex responses to muscle stretch. *J Physiol* 292: 527–534, 1979.

Conrad B, Brooks VB. Effects of dentate cooling on rapid alternating arm movements. *J Neurophysiol* 37: 792–804, 1974.

Crago PE, Houk JC, Hasan Z. Regulatory actions of human stretch reflex. *J Neurophysiol* 39: 925–935, 1976.

Crevecoeur F, Kurtzer I, Scott SH. Fast corrective responses are evoked by perturbations approaching the natural variability of posture and movement tasks. *J Neurophysiol* 107: 2821–2832, 2012.

Crevecoeur F, Scott SH. Priors engaged in long-latency responses to mechanical perturbations suggest a rapid update in state estimation. *PLoS Comput Biol* 9: e1003177, 2013.

Diedrichsen J, Criscimagna-Hemminger SE, Shadmehr R. Dissociating timing and coordination as functions of the cerebellum. *J Neurosci* 27: 6291–6301, 2007.

Dietz V, Dicher M, Trippel M. Task-dependent modulation of short-latency and long-latency electromyographic responses in upper-limb muscles. *Electroencephalogr Clin Neurophysiol* 93: 49–56, 1994.

Dimitriou M, Franklin DW, Wolpert DM. Task-dependent coordination of rapid bimanual motor responses. *J Neurophysiol* 107: 890–901, 2012.

Doemges F, Rack PM. Changes in the stretch reflex of the human first dorsal interosseous muscle during different tasks. *J Physiol* 447: 563–573, 1992a.

Doemges F, Rack PM. Task-dependent changes in the response of human wrist joints to mechanical disturbance. *J Physiol* 447: 575–585, 1992b.

Duysens J, Tax AA, Dietz MT. Increased amplitude of cutaneous reflexes during human running as compared to standing. *Brain Res* 613: 230–238, 1993.

Evarts EV, Fromm C. Sensory responses in motor cortex neurons during precise motor control. *Neurosci Lett* 5: 267–272, 1977.

Evarts EV, Granit R. Relations of reflexes and intended movements. *Prog Brain Res* 44: 1–14, 1976.

Evarts EV, Tanji J. Reflex and intended responses in motor cortex pyramidal tract neurons of monkey. *J Neurophysiol* 39: 1069–1080, 1976.

Fetz EE, Cheney PD. Postspike facilitation of forelimb muscle activity by primate corticomotoneuronal cells. *J Neurophysiol* 44: 751–772, 1980.

Forssberg H, Grillner S, Rossignol S. Phase dependent reflex reversal during walking in chronic spinal cats. *Brain Res* 85: 103–107, 1975.

Gielen CC, Ramaekers L, van Zuylen EJ. Long-latency stretch reflexes as co-ordinated functional responses in man. *J Physiol* 407: 275–292, 1988.

Gottlieb GL, Agarwal GC. Response to sudden torques about ankle in man: myotatic reflex. *J Neurophysiol* 42: 91–106, 1979.

Green DM, Swets JA. *Signal Detection and Recognition by Human Observers*. New York: Wiley, 1966.

Grey MJ, Ladouceur M, Andersen JB, Nielsen JB, Sinkjaer T. Group II muscle afferents probably contribute to the medium latency soleus stretch reflex during walking in humans. *J Physiol* 534: 925–933, 2001.

Gribble PL, Ostry DJ. Compensation for interaction torques during single- and multijoint limb movement. *J Neurophysiol* 82: 2310–2326, 1999.

Hager-Ross C, Cole KJ, Johansson RS. Grip-force responses to unanticipated object loading: load direction reveals body- and gravity-referenced intrinsic task variables. *Exp Brain Res* 110: 142–150, 1996.

Hammond PH. The influence of prior instruction to the subject on an apparently involuntary neuro-muscular response. *J Physiol* 132: 17P–18P, 1956.

Hore J, Vilis T. Loss of set in muscle responses to limb perturbations during cerebellar dysfunction. *J Neurophysiol* 51: 1137–1148, 1984.

Hore J, Watts S. Skilled throwers use physics to time ball release to the nearest millisecond. *J Neurophysiol* 106: 2024–2033, 2011.

Ingram DA, Davis GR, Swash M. Motor nerve conduction velocity distributions in man: results of a new computer-based collision technique. *Electroencephalogr Clin Neurophysiol* 66: 235–243, 1987.

Ivry RB, Keele SW. Timing functions of the cerebellum. *J Cogn Neurosci* 2: 136–152, 1989.

Jaeger RJ, Gottlieb GL, Agarwal GC. Myoelectric responses at flexors and extensors of human wrist to step torque perturbations. *J Neurophysiol* 48: 388–402, 1982.

Johansson AS, Pruszynski JA, Edin BB, Westberg KG. Biting intentions modulate digastric reflex responses to sudden unloading of the jaw. *J Neurophysiol* 112: 1067–1073, 2014.

Karst GM, Hasan Z. Timing and magnitude of electromyography activity for two-joint arm movements in different directions. *J Neurophysiol* 66: 1594–1604, 1991

Kimura T, Haggard P, Gomi H. Transcranial magnetic stimulation over sensorimotor cortex disrupts anticipatory reflex gain modulation for skilled action. *J Neurosci* 26: 9272–9281, 2006.

Komiyama T, Zehr EP, Stein RB. Absence of nerve specificity in human cutaneous reflexes during standing. *Exp Brain Res* 133: 267–272, 2000.

Koshland GF, Hasan Z, Gerilovsky L. Activity of wrist muscles elicited during imposed or voluntary movements about the elbow joint. *J Mot Behav* 23: 91–100, 1991.

Krutky MA, Ravichandran VJ, Trumbower RD, Perreault EJ. Interactions between limb and environmental mechanics influence stretch reflex sensitivity in the human arm. *J Neurophysiol* 103: 429–440, 2010.

Kurtzer IL, Crevecoeur F, Scott SH. Fast feedback control involves two independent processes utilizing knowledge of limb dynamics. *J Neurophysiol* 111: 1631–1645, 2014.

Kurtzer IL, Pruszynski JA, Scott SH. Long-latency reflexes of the human arm reflect an internal model of limb dynamics. *Curr Biol* 18: 449–453, 2008.

Kurtzer IL, Pruszynski JA, Scott SH. Long-latency responses during reaching account for the mechanical interaction between the shoulder and elbow joints. *J Neurophysiol* 102: 3004–3015, 2009.

Kurtzer I, Pruszynski JA, Scott SH. Long-latency responses to an arm displacement can be rapidly attenuated by perturbation offset. *J Neurophysiol* 103: 3195–3204, 2010.

Kurtzer IL, Trautman P, Rasquinha RJ, Bhanpuri NH, Scott SH, Bastian AJ. Cerebellar damage diminishes long-latency responses to multijoint perturbations. *J Neurophysiol* 109: 2228–2241, 2013.

Lee RG, Tatton WG. Long latency reflexes to imposed displacements of the human wrist: dependence on duration of movement. *Exp Brain Res* 45: 207–216, 1982.

Lourenço G, Iglesias C, Cavallari P, Pierrot-Deseilligny E, Marchand-Pauvert V. Mediation of late excitation from human hand muscles via parallel group II spinal and group I transcortical pathways. *J Physiol* 572: 585–603, 2006.

Ludvig D, Cathers I, Kearney RE. Voluntary modulation of human stretch reflexes. *Exp Brain Res* 183: 201–213, 2007.

Macefield G, Gandevia SC, Burke D. Conduction velocities of muscle and cutaneous afferents in the upper and lower limbs of human subjects. *Brain* 112: 1519–1532, 1989.

Manning CD, Tolhurst SA, Bawa P. Proprioceptive reaction times and long-latency reflexes in humans. *Exp Brain Res* 221: 155–166, 2012.

Marsden CD, Merton PA, Morton HB. Human postural responses. *Brain* 104: 513–534, 1981.

Matthews PB. Evidence from the use of vibration that the human long-latency stretch reflex depends upon spindle secondary afferents. *J Physiol* 348: 383–415, 1984.

Matthews PB. The human stretch reflex and the motor cortex. *Trends Neurosci* 14: 87–91, 1991.

Matthews PB, Miles TS. On the long-latency reflex responses of the human flexor digitorum profundus. *J Physiol* 404: 515–534, 1988.

McKiernan BJ, Marcario JK, Karrer JH, Cheney PD. Corticomotoneuronal postspike effects in shoulder, elbow, wrist, digit, and intrinsic hand muscles during a reach and prehension task. *J Neurophysiol* 80: 1961–1980, 1998.

Mortimer JA, Webster DD, Dukich TG. Changes in short and long latency stretch responses during the transition from posture to movement. *Exp Brain Res* 229: 337–351, 1981.

Mutha PK, Sainburg RL. Shared bimanual tasks elicit bimanual reflexes during movement. *J Neurophysiol* 102: 3142–3155, 2009.

Nashed JY, Crevecoeur F, Scott SH. Influence of the behavioral goal and environmental obstacles on rapid feedback responses. *J Neurophysiol* 108: 999–1009, 2012.

Nashed JY, Crevecoeur F, Scott SH. Rapid online selection between multiple motor plans. *J Neurosci* 29: 1769–1780, 2014.

Ohki Y, Johansson RS. Sensorimotor interactions between pairs of fingers in bimanual and unimanual manipulative tasks. *Exp Brain Res* 127: 43–53, 1999.

Omrani M, Diedrichsen J, Scott SH. Rapid feedback corrections during a bimanual postural task. *J Neurophysiol* 109: 147–161, 2013.

Omrani M, Pruszynski JA, Murnaghan CD, Scott SH. Perturbation-evoked responses in primary motor cortex are modulated by behavioral context. *J Neurophysiol* 112: 2985–3000, 2014.

Perreault EJ, Chen K, Trumbower RD, Lewis G. Interactions with compliant loads alter stretch reflex gains but not intermuscular coordination. *J Neurophysiol* 99: 2101–2113, 2008.

Picard N, Smith AM. Primary motor cortical responses to perturbations of prehension in the monkey. *J Neurophysiol* 68: 1882–1894, 1992.

Pierrot-Deseilligny E, Burke D. *The Circuitry of the Spinal Cord: Its Role in Motor Control and Movement Disorders*. Cambridge, UK: Cambridge Univ. Press, 2005.

Pruszynski JA. Primary motor cortex and fast feedback responses to mechanical perturbations: a primer on what we know now and some suggestions on what we should find out next. *Front Integr Neurosci* 8: 72, 2014.

Pruszynski JA, Kurtzer I, Lillicrap TP, Scott SH. Temporal evolution of "automatic gain-scaling." *J Neurophysiol* 102: 992–1003, 2009.

Pruszynski JA, Kurtzer I, Nashed JY, Omrani M, Brouwer B, Scott SH. Primary motor cortex underlies multi-joint integration for fast feedback control. *Nature* 478: 387–390, 2011a.

Pruszynski JA, Kurtzer I, Scott SH. Rapid motor responses are appropriately tuned to the metrics of a visuospatial task. *J Neurophysiol* 100: 224–238, 2008.

Pruszynski JA, Kurtzer I, Scott SH. The long-latency reflex is composed of at least two functionally independent processes. *J Neurophsyiol* 106: 449–459, 2011b.

Pruszynski JA, Omrani M, Scott SH. Goal-dependent modulation of fast feedback responses in primary motor cortex. *J Neurosci* 34: 4608–4617, 2014.

Pruszynski JA, Scott SH. Optimal feedback control and the long-latency stretch response. *Exp Brain Res* 218: 341–359, 2012.

Raphael G, Tsianos GA, Loeb GE. Spinal-like regulator facilitates control of a two-degree-of-freedom wrist. *J Neurosci* 30: 9431–9444, 2010.

Ravichandran VJ, Honeycutt CF, Shemmell J, Perreault EJ. Instruction-dependent modulation of the long-latency stretch reflex is associated with indicators of startle. *Exp Brain Res* 230: 59–69, 2013.

Rothwell JC, Traub MM, Marsden CD. Influence of voluntary intent on the human long-latency stretch reflex. *Nature* 286: 496–498, 1980.

Scholz JP, Schöner G, Latash ML. Identifying the control structure of multijoint coordination during pistol shooting. *Exp Brain Res* 135: 382–404, 2000.

Schuurmans J, de Vlugt E, Schouten AC, Meskers CG, de Groot JH, van der Helm FC. The monosynaptic Ia afferent pathway can largely explain the stretch duration effect of the long latency M2 response. *Exp Brain Res* 193: 491–500, 2009.

Scott SH. Optimal feedback control and the neural basis of volitional motor control. *Nat Rev Neurosci* 5: 532–546, 2004.

Selen LP, Shadlen MN, Wolpert DM. Deliberation in the motor system: reflex gains track evolving evidence leading to a decision. *J Neurosci* 32: 2276–2286, 2012.

Shemmell J, An JH, Perreault EJ. The differential role of motor cortex in stretch reflex modulation induced by changes in environmental mechanics and verbal instruction. *J Neurosci* 29: 13255–13263, 2009.

Shemmell J, Krutky MA, Perreault EJ. Stretch sensitivity reflexes as an adaptive mechanism for maintaining limb stability. *Clin Neurophysiol* 121: 1680–1689. 2010.

Soechting JF, Lacquaniti F. Quantitative evaluation of the electromyographic responses to multidirectional load perturbations of the human arm. *J Neurophysiol* 59: 1296–1313, 1988.

Strick PL. The influence of motor preparation on the response of cerebellar neurons to limb displacements. *J Neurosci* 3: 2007–2020, 1983.

Thompson AK, Chen XY, Wolpaw JR. Acquisition of a simple motor skill: task-dependent adaptation plus long-term change in the human soleus H-reflex. *J Neurosci* 29: 5784–5792, 2009.

Thompson AK, Pomerantz FR, Wolpaw JR. Operant conditioning of a spinal reflex can improve locomotion after spinal cord injury in humans. *J Neurosci* 33: 2365–2375, 2013.

Todorov E, Jordan MI. Optimal feedback control as a theory of motor control. *Nat Neurosci* 5: 1226–1235, 2002.

Vilis T, Hore J. Central neural mechanisms contributing to cerebellar tremor produced by limb perturbations. *J Neurophysiol* 43: 279–291, 1980.

Wolf SL, Segal RL. Reducing human biceps brachii spinal stretch reflex magnitude. *J Neurophysiol* 75: 1637–1646, 1996.

Wolpaw JR. Amplitude of responses to perturbation in primate sensorimotor cortex as a function of task. *J Neurophysiol* 44: 1139–1147, 1980.

Wolpaw JR. Operant conditioning of primate spinal reflexes: the H-reflex. *J Neurophysiol* 57: 443–459, 1987.

Wolpaw JR, Braitman DJ, Seegal RF. Adaptive plasticity in primate spinal stretch reflex: initial development. *J Neurophysiol* 50: 1296–1311, 1983.

Yang L, Michaels JA, Pruszynski JA, Scott SH. Rapid motor responses quickly integrate visuospatial task constraints. *Exp Brain Res* 211: 231–242, 2011.

Zehr EP, Chua R. Modulation of human cutaneous reflexes during rhythmic cyclical arm movement. *Exp Brain Res* 135: 241–250, 2000.

Zehr EP, Haridas C. Modulation of cutaneous reflexes in arm muscles during walking: further evidence of similar control mechanisms for rhythmic human arm and leg movements. *Exp Brain Res* 149: 260–266, 2003.